



SUPPLEMENTARY MATERIAL TO

**Redox properties of alkyl-substituted 4-aryl-2,4-dioxobutanoic acids**

ILIJA N. CVIJETIĆ<sup>1</sup>, TATJANA Ž. VERBIĆ<sup>2\*</sup>, **BRANKO J. DRAKULIĆ<sup>3\*\*</sup>**, DALIBOR M. STANKOVIĆ<sup>1,4</sup>, IVAN O. JURANIĆ<sup>3</sup>, DRAGAN D. MANOJLOVIĆ<sup>2</sup> and MIRE ZLOH<sup>5</sup>

<sup>1</sup>Innovation Center of the Faculty of Chemistry, University of Belgrade, Studentski Trg 16, 11000 Belgrade, Serbia, <sup>2</sup>Faculty of Chemistry, University of Belgrade, Studentski Trg 16, 11000 Belgrade, Serbia, <sup>3</sup>Institute of Chemistry, Technology and Metallurgy, Department of Chemistry, University of Belgrade, Njegoševa 12, 11000 Belgrade, Serbia, <sup>4</sup>Vinča Institute of Nuclear Sciences, University of Belgrade, P. O. Box 522, 11001 Belgrade, Serbia and <sup>5</sup>Department of Pharmacy, University of Hertfordshire, Hatfield, Hertfordshire AL10 9AB, United Kingdom

J. Serb. Chem. Soc. 82 (3) (2017) 303–316

*2,4-Dioxo-4-phenylbutanoic acid (1)*. Yield: 7.90 g, 80 %; pale yellow powder; m.p.: 142–143 °C, dcc\*\* (from AcOEt/benzene); C<sub>10</sub>H<sub>8</sub>O<sub>4</sub>, FW: 192.17; IR (ATR, cm<sup>-1</sup>): 2997 *br* (COO–H st), 1720 (C=O st), 1626 (C=O st\*\*\*), 1275 (C–O st); <sup>1</sup>H-NMR (200 MHz, DMSO-*d*<sub>6</sub>, δ / ppm): 13.55 (1H, *s*, COOH), 8.00 (2H, *d*, *J* = 8.4 Hz, *o*-H), 7.65 (1H, *t*, *J* = 7.3 Hz, *p*-H), 7.51 (2H, *t*, *J* = 7.3 Hz, *m*-H), 7.32 (1H, *s*, probably from CH of the less abundant enol form), 7.08 (1H, *s*, CH of the enol form), 4.57 (1H, *bs*, CH<sub>2</sub> of the diketo form); <sup>13</sup>C-NMR (50 MHz, DMSO-*d*<sub>6</sub>, δ / ppm): 190.88, 170.60, 163.56, 134.97, 134.33, 129.43, 129.22, 128.83, 128.68, 128.20, 98.21, 49.60. Two tautomeric forms were visible in DMSO solution, and the signal at 49.60 ppm corresponds to the methylene group of the diketo tautomer.

*4-(2-Methylphenyl)-2,4-dioxobutanoic acid (2)*. Yield: 1.25 g, 76 %; white solid; m.p.: 106–108 °C, dcc (from EtOH); C<sub>11</sub>H<sub>10</sub>O<sub>4</sub>, FW: 206.19; IR (ATR, cm<sup>-1</sup>): 2991 *br* (COO–H st), 1710 (C=O st), 1635 (C=O st), 1279 (C–O st); <sup>1</sup>H-NMR (200 MHz, DMSO-*d*<sub>6</sub>, δ / ppm): 7.68 (1H, *d*, *J* = 8.4 Hz, *o*-H), 7.48 (1H, *t*, *J* = 7.3 Hz, *m*-H), 7.35 (1H, *t*, *p*-H), overlapped with 7.31 (1H, *d*, *J* = Hz, *m*-H), 6.71 (1H, *s*, CH of enol form), 4.48 (*bs*, CH<sub>2</sub> of diketo form), 2.45 (3H, *s*, CH<sub>3</sub>); <sup>13</sup>C-NMR (50 MHz, DMSO-*d*<sub>6</sub>, δ / ppm): 194.66, 168.48, 163.35, 137.50,

\* Corresponding author. E-mail: tatjanad@chem.bg.ac.rs

\*\*Decomposition; \*\*\* stretching

135.86, 132.13, 131.83, 129.04, 126.32, 101.69, 51.78, 20.62; ESI-HR/MS: Calcd. for  $C_{11}H_9O_4$  (M-H): 205.0501. Found: 205.0509.

*4-(3-Methylphenyl)-2,4-dioxobutanoic acid (3)*. Yield: 0.82 g, 73 %; white solid; m.p.: 98–99 °C (from EtOH),  $C_{11}H_{10}O_4$ , FW: 206.19; IR (ATR,  $cm^{-1}$ ): 3501 *br* (COO-H st), 1683 (C=O st), 1628 (C=O st), 1257 (C-O st);  $^1H$ -NMR (200 MHz, DMSO- $d_6$ ,  $\delta$  / ppm): 7.84 (1H, *s*, *o*-H), 7.80 (1H, *d*,  $J = 8.0$  Hz, *o*-H), 7.45 (1H, *d*,  $J = 8.0$  Hz, *p*-H), 7.41 (1H, *t*,  $J = 8.0$  Hz, *m*-H), 7.06 (1H, *s*, CH of enol form), 4.53 (*bs*,  $CH_2$  of diketo form), 2.36 (3H, *s*,  $CH_3$ );  $^{13}C$ -NMR (50 MHz, DMSO- $d_6$ ,  $\delta$  / ppm): 190.70, 170.30, 163.30, 138.72, 134.78, 134.70, 129.08, 128.30, 125.15, 97.95, 53.13, 20.84; ESI-HR/MS: Calcd. for  $C_{11}H_9O_4$  (M-H): 205.0501. Found: 205.0508.

*4-(4-Methylphenyl)-2,4-dioxobutanoic acid (4)*. Yield: 6.30 g, 61 %; light yellow crystals; m.p.: 140–141 °C (from AcOEt/PhMe);  $C_{11}H_{10}O_4$ , FW: 206.19; IR (ATR,  $cm^{-1}$ ): 3520 *br* (COO-H st), 1603 (C=O st), 1248 (C-O st);  $^1H$ -NMR (500 MHz,  $CD_3OD$ ,  $\delta$  / ppm): 7.93 (2H, *d*,  $J = 8.2$  Hz,  $2 \times$  *o*-H), 7.85 (less abundant tautomer, *d*,  $J = 8.2$  Hz), 7.35 (2H, *d*,  $J = 8.0$  Hz,  $2 \times$  *m*-H), 7.30 (less abundant tautomer, *d*,  $J = 8.0$  Hz), 7.09 (1H, *s*, CH of enol form), 2.41 (3H, *s*,  $CH_3$ );  $^{13}C$ -NMR (125 MHz,  $CD_3OD$ ,  $\delta$  / ppm): 191.98, 171.05, 165.15, 146.49, 133.91, 130.68, 129.20, 98.77, 21.84.

*4-(2,4-Dimethylphenyl)-2,4-dioxobutanoic acid (5)*. Yield: 5.21 g, 78 %; pale yellow solid; m.p.: 123–124 °C (from AcOEt/PhMe);  $C_{12}H_{12}O_4$ , FW: 220.22; IR (ATR,  $cm^{-1}$ ): 2969 *br* (COO-H st), 1710 (C=O st), 1633 (C=O st), 1271 (C-O st);  $^1H$ -NMR (200 MHz,  $CDCl_3$ ,  $\delta$  / ppm): 7.60 (1H, *d*,  $J = 8.4$  Hz, *o*-H), 7.11–7.15 (2H, *m*, overlapped *d* and *s* from  $2 \times$  *m*-H), 6.96 (1H, *s*, CH of enol form), 2.55 (3H, *s*,  $CH_3$ ), 2.38 (3H, *s*,  $CH_3$ );  $^{13}C$ -NMR (50 MHz,  $CDCl_3$ ,  $\delta$  / ppm): 194.32, 168.65, 164.85, 143.78, 139.32, 133.24, 131.90, 129.81, 127.02, 100.92, 21.59; ESI-HR/MS: Calcd. for  $C_{12}H_{11}O_4$  (M-H): 219.0657. Found: 219.0663.

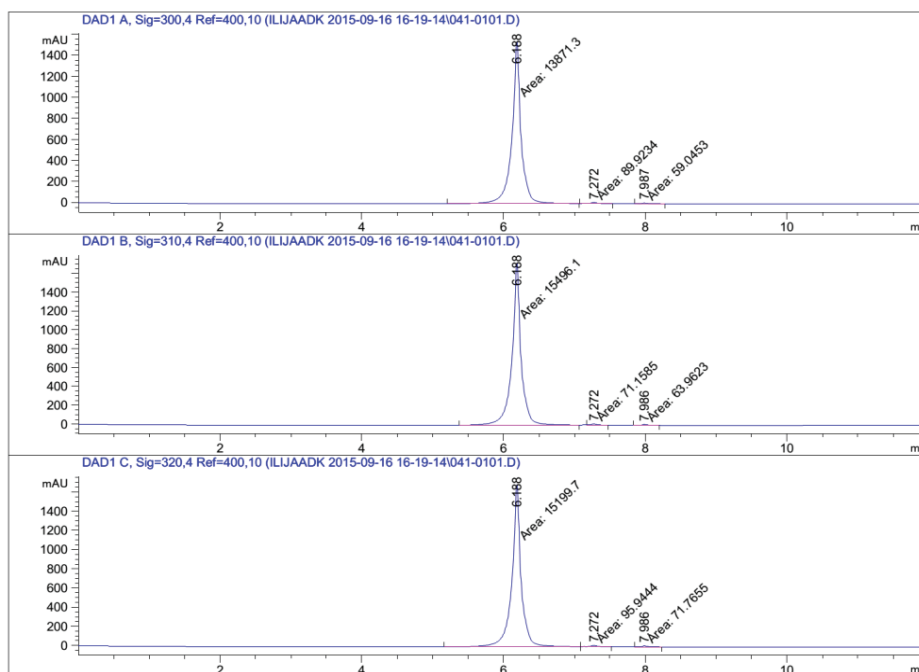
*4-(2,5-Dimethylphenyl)-2,4-dioxobutanoic acid (6)*. Yield: 7.93 g, 72 %; white powder; m.p.: 150–152 °C (from AcOEt/PhMe);  $C_{12}H_{12}O_4$ , FW: 220.22; IR (ATR,  $cm^{-1}$ ): 2969 *br* (COO-H st), 1701 (C=O st), 1619 (C=O st), 1292 (C-O st);  $^1H$ -NMR (200 MHz, DMSO- $d_6$ ,  $\delta$  / ppm): 7.76 (1H, *s*, *o*-H), 7.71 (1H, *d*,  $J = 8.1$  Hz, *p*-H), 7.28 (1H, *d*,  $J = 7.9$  Hz, *m*-H), 6.65 (1H, *bs*, CH of enol form), 4.40 (*bs*,  $CH_2$  of diketo form), 2.29 (6H, *s*,  $2 \times$   $CH_3$ );  $^{13}C$ -NMR (50 MHz, DMSO- $d_6$ ,  $\delta$  / ppm): 164.36, 137.00, 133.28, 130.00, 128.36, 125.10, 97.88, 19.61, 19.37.

*4-(3,4-Dimethylphenyl)-2,4-dioxobutanoic acid (7)*. Yield: 6.30 g, 57 %; white powder; m.p.: 175–177 °C, *dcc* (from AcOEt/PhMe);  $C_{12}H_{12}O_4$ , FW: 220.22; IR (ATR,  $cm^{-1}$ ): 3474 *br* (COO-H st), 1705 (C=O st), 1612 (C=O st), 1261 (C-O st);  $^1H$ -NMR (200 MHz, DMSO- $d_6$ ,  $\delta$  / ppm): 7.78 (1H, *s*, *o*-H), 7.73 (1H, *d*,  $J = 8.1$  Hz, *o*-H), 7.29 (1H, *d*,  $J = 7.9$  Hz, *m*-H), 6.77 (1H, *bs*, CH of enol

form), 4.43 (*bs*, CH<sub>2</sub> of diketo form), 2.29 (6H, *s*, 2× CH<sub>3</sub>); <sup>13</sup>C-NMR (50 MHz, DMSO-*d*<sub>6</sub>, δ / ppm): 164.23, 142.62, 137.15, 133.09, 130.11, 128.49, 125.27, 97.73, 19.65, 19.36.

*2,4-Dioxo-4-(2,4,5-trimethylphenyl)butanoic acid (8)*. Yield: 4.58 g, 68 %; pale yellow solid; m.p.: 139–141 °C (from AcOEt/PhMe); C<sub>13</sub>H<sub>14</sub>O<sub>4</sub>, FW: 234.25; IR (ATR, cm<sup>-1</sup>): 2925 *br* (COO–H st), 1709 (C=O st), 1619 (C=O st), 1275 (C–O st); <sup>1</sup>H-NMR (200 MHz, DMSO-*d*<sub>6</sub>, δ / ppm): 7.52 (1H, *s*, *o*-H), 7.10 (1H, *s*, *m*-H), 6.80 (1H, *s*, CH of enol form), 4.47 (*bs*, CH<sub>2</sub> of diketo form), 2.43 (3H, *s*, CH<sub>3</sub>), 2.24 (6H, *s*, 2× CH<sub>3</sub>); <sup>13</sup>C-NMR (50 MHz, DMSO-*d*<sub>6</sub>, δ / ppm): 195.23, 167.80, 163.43, 141.66, 135.50, 134.29, 133.27, 132.81, 130.31, 101.23, 51.46, 20.52, 19.35, 18.65. Two tautomeric forms are visible in DMSO solution, and the signal at 51.46 ppm corresponds to the methylene group of the diketo tautomer; ESI-HR/MS: Calcd. for C<sub>13</sub>H<sub>13</sub>O<sub>4</sub> (M–H): 233.0819. Found: 233.0821.

*2,4-Dioxo-4-(2,3,5,6-tetramethylphenyl)butanoic acid (9)*. Yield: 5.20 g, 78 %; white solid; m.p.: 156–158 °C *dec*, (from AcOEt/PhMe); C<sub>14</sub>H<sub>16</sub>O<sub>4</sub>, FW: 248.27; IR (ATR, cm<sup>-1</sup>): 2962 *br* (COO–H st), 1743 (C=O st), 1599 (C=O st), 1261 (C–O st); <sup>1</sup>H-NMR (200 MHz, DMSO-*d*<sub>6</sub>, δ / ppm): 6.96 (1H, *s*, *p*-H), 6.21 (1H, *s*, CH of enol form), 2.13 (6H, *s*, 2× CH<sub>3</sub>), 2.04 (6H, *s*, 2× CH<sub>3</sub>); <sup>13</sup>C-NMR (50 MHz, DMSO-*d*<sub>6</sub>, δ / ppm): 196.89, 169.17, 163.77, 138.70, 133.87, 132.00, 129.19, 103.77, 19.29, 15.98; ESI-HR/MS: Calcd. for C<sub>14</sub>H<sub>15</sub>O<sub>4</sub> (M–H): 247.0976. Found: 247.0976.



Signal 1: DAD1 A, Sig=300,4 Ref=400,10						Signal 2: DAD1 B, Sig=310,4 Ref=400,10							
Peak #	RetTime [min]	Type	Width [min]	Area [mAU*s]	Height [mAU]	Area %	Peak #	RetTime [min]	Type	Width [min]	Area [mAU*s]	Height [mAU]	Area %
1	6.188	MM	0.1499	1.38713e4	1542.77527	98.9375	1	6.188	MM	0.1498	1.54961e4	1723.59949	99.1356
2	7.272	MM	0.1237	89.92340	12.11744	0.6414	2	7.272	MM	0.0992	71.15846	11.95799	0.4552
3	7.987	MM	0.1303	59.04533	7.55190	0.4211	3	7.986	MM	0.1170	63.96226	9.10771	0.4092
Totals :				1.40203e4	1562.44460		Totals :				1.56312e4	1744.66518	

Signal 3: DAD1 C, Sig=320,4 Ref=400,10						
Peak #	RetTime [min]	Type	Width [min]	Area [mAU*s]	Height [mAU]	Area %
1	6.188	MM	0.1498	1.51997e4	1690.71960	98.9087
2	7.272	MM	0.1266	95.94437	12.63321	0.6243
3	7.986	MM	0.1167	71.76546	10.25321	0.4670
Totals :				1.53674e4	1713.60602	

Fig. S-1. Chromatogram for the assessment of the purity of compound **1**, with tables showing the detector response at three wavelengths.

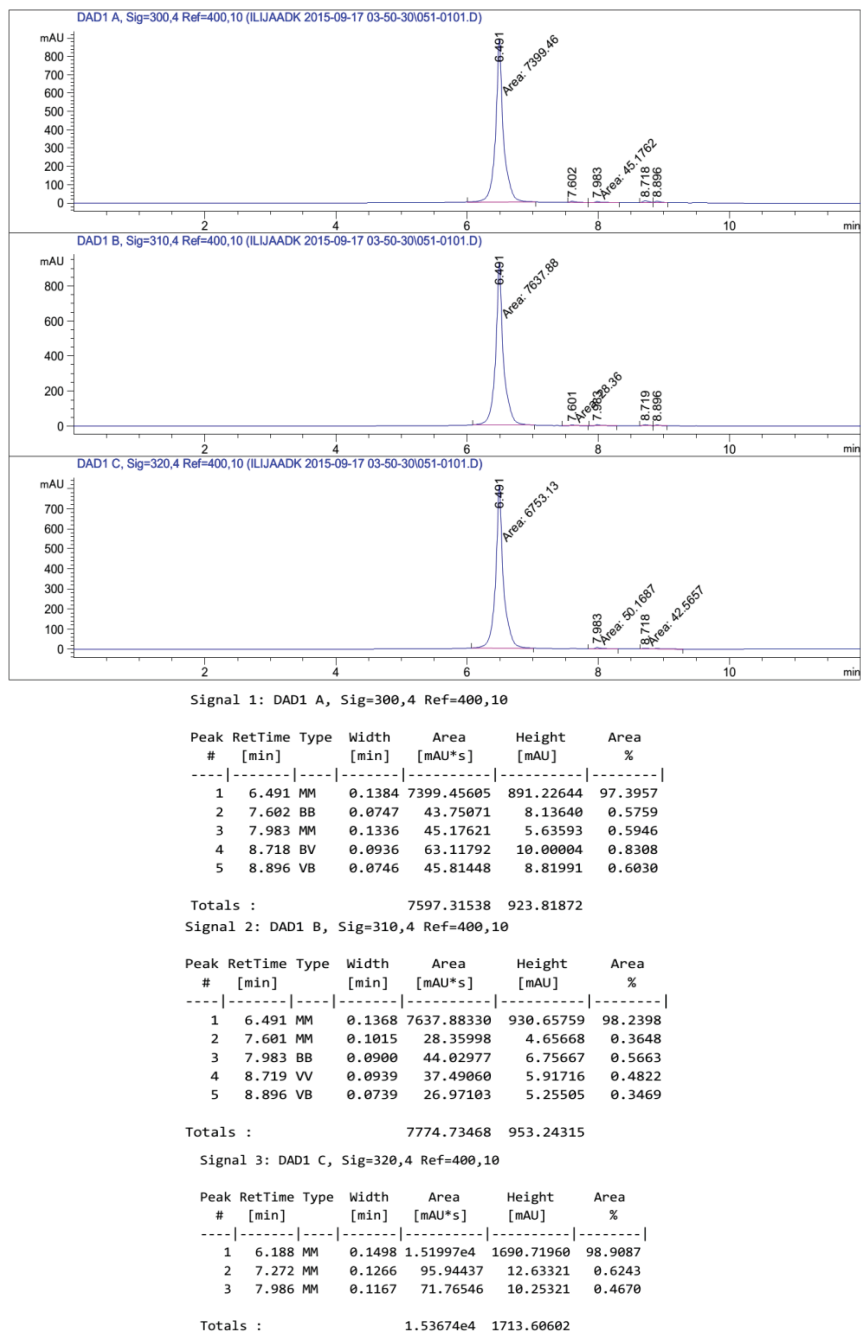
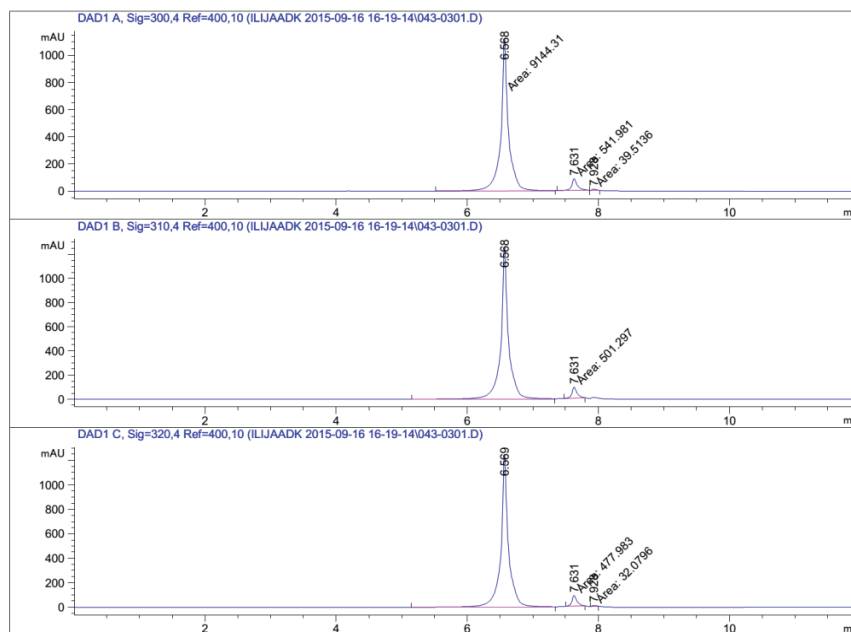


Fig. S-2. Chromatogram for the assessment of the purity of compound 2, with tables showing the detector response at three wavelengths.



Signal 1: DAD1 A, Sig=300,4 Ref=400,10

Peak #	RetTime [min]	Type	Width [min]	Area [mAU*s]	Height [mAU]	Area %
1	6.568	MM	0.1354	9144.30762	1125.57922	94.0211
2	7.631	MM	0.1035	541.98132	87.25426	5.5726
3	7.928	MM	0.0752	39.51355	8.76017	0.4063

Totals : 9725.80249 1221.59366

Signal 2: DAD1 B, Sig=310,4 Ref=400,10

Peak #	RetTime [min]	Type	Width [min]	Area [mAU*s]	Height [mAU]	Area %
1	6.568	BV	0.1105	1.04653e4	1265.41760	95.4289
2	7.631	MM	0.0912	501.29694	91.58324	4.5711

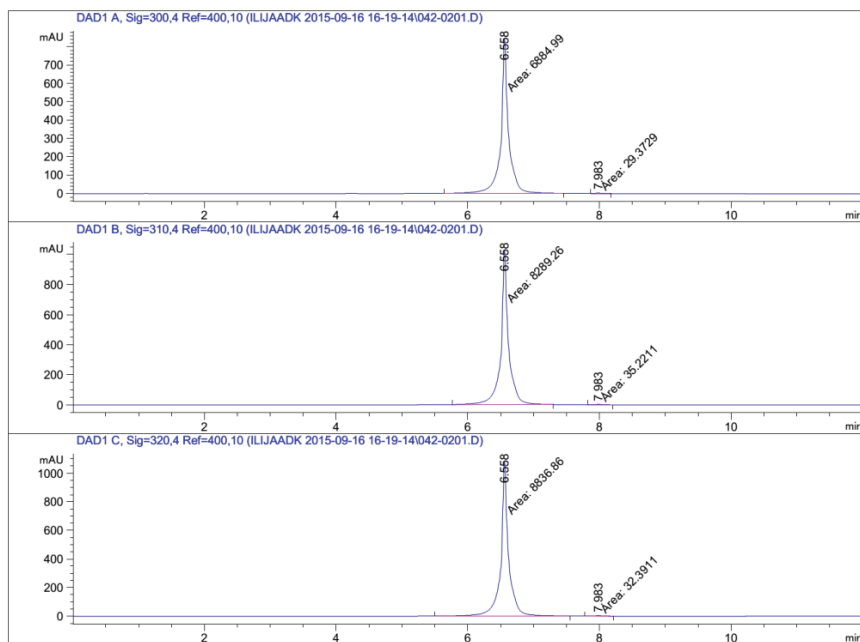
Totals : 1.09666e4 1357.00084

Signal 3: DAD1 C, Sig=320,4 Ref=400,10

Peak #	RetTime [min]	Type	Width [min]	Area [mAU*s]	Height [mAU]	Area %
1	6.569	BV	0.1125	1.03210e4	1247.92981	95.2907
2	7.631	MM	0.0909	477.98343	87.68449	4.4131
3	7.928	MM	0.0651	32.07959	8.20785	0.2962

Totals : 1.08310e4 1343.82214

Fig. S-3. Chromatogram for the assessment of the purity of compound 3, with tables showing the detector response at three wavelengths.



Signal 1: DAD1 A, Sig=300,4 Ref=400,10

Peak #	RetTime [min]	Type	Width [min]	Area [mAU*s]	Height [mAU]	Area %
1	6.558	MM	0.1359	6884.98584	844.67102	99.5752
2	7.983	MM	0.1335	29.37285	3.66623	0.4248

Totals : 6914.35869 848.33725

Signal 2: DAD1 B, Sig=310,4 Ref=400,10

Peak #	RetTime [min]	Type	Width [min]	Area [mAU*s]	Height [mAU]	Area %
1	6.558	MM	0.1343	8289.25977	1029.00488	99.5769
2	7.983	MM	0.1359	35.22105	4.31915	0.4231

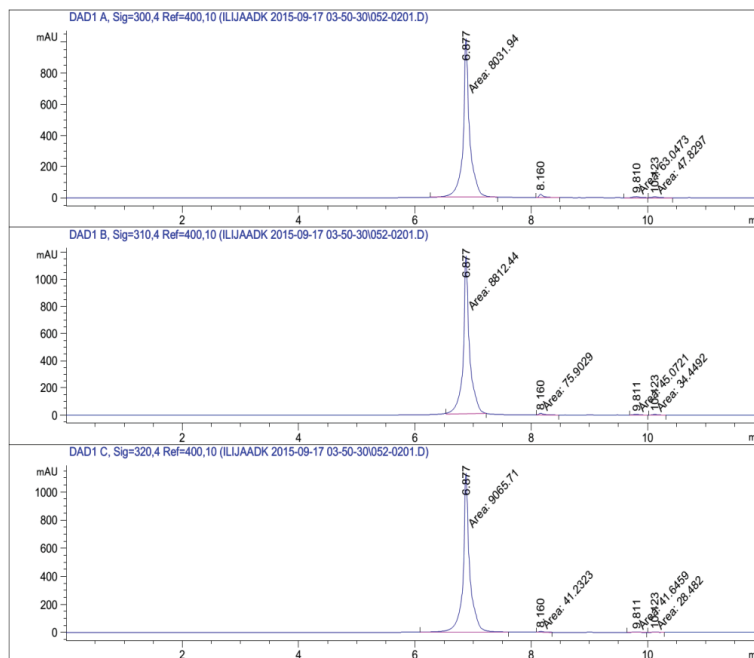
Totals : 8324.48082 1033.32404

Signal 3: DAD1 C, Sig=320,4 Ref=400,10

Peak #	RetTime [min]	Type	Width [min]	Area [mAU*s]	Height [mAU]	Area %
1	6.558	MM	0.1359	8836.85742	1083.69934	99.6348
2	7.983	MM	0.1194	32.39113	4.52258	0.3652

Totals : 8869.24855 1088.22192

Fig. S-4. Chromatogram for the assessment of the purity of compound **4**, with tables showing the detector response at three wavelengths.



Signal 1: DAD1 A, Sig=300,4 Ref=400,10

Peak #	RetTime [min]	Type	Width [min]	Area [mAU*s]	Height [mAU]	Area %
1	6.877	MM	0.1312	8031.94043	1020.67456	97.2473
2	8.160	BV	0.0785	116.47652	21.05224	1.4102
3	9.810	MM	0.1373	63.04733	7.65068	0.7634
4	10.123	MM	0.1081	47.82969	7.37333	0.5791

Totals : 8259.29396 1056.75080

Signal 2: DAD1 B, Sig=310,4 Ref=400,10

Peak #	RetTime [min]	Type	Width [min]	Area [mAU*s]	Height [mAU]	Area %
1	6.877	MM	0.1261	8812.43652	1164.66846	98.2669
2	8.160	MM	0.0959	75.90292	13.19241	0.8464
3	9.811	MM	0.1394	45.07211	5.38910	0.5026
4	10.123	MM	0.1095	34.44922	5.24225	0.3841

Totals : 8967.86077 1188.49222

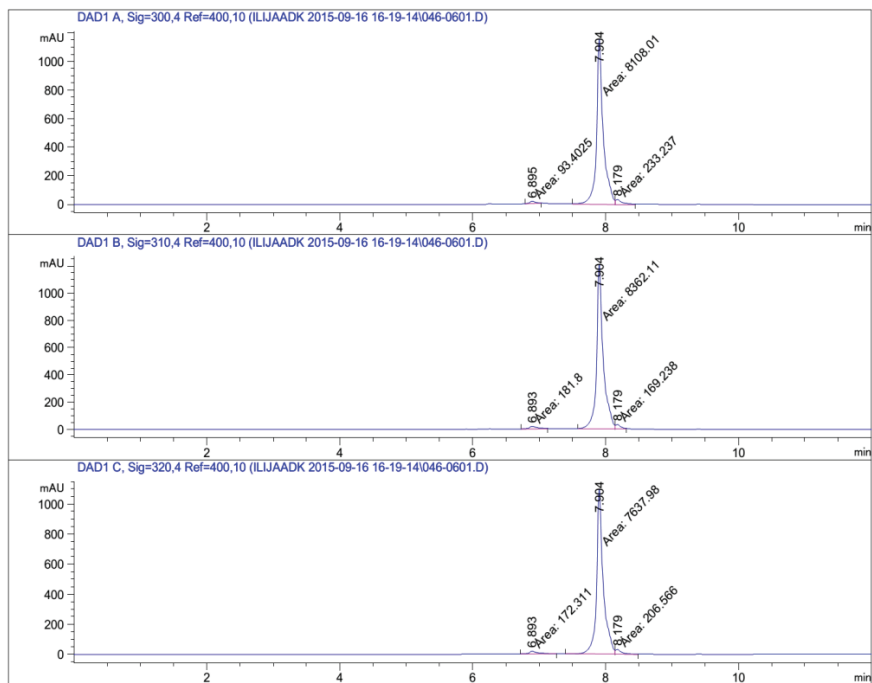
Signal 3: DAD1 C, Sig=320,4 Ref=400,10

Peak #	RetTime [min]	Type	Width [min]	Area [mAU*s]	Height [mAU]	Area %
1	6.877	MM	0.1330	9065.71289	1136.19385	98.7865
2	8.160	MM	0.0936	41.23225	7.34139	0.4493
3	9.811	MM	0.1716	41.64587	4.04555	0.4538
4	10.123	MM	0.1264	28.48196	3.75556	0.3104

Totals : 9177.07297 1151.33635

Fig. S-5. Chromatogram for the assessment of the purity of compound 5, with tables showing the detector response at three wavelengths.





Signal 1: DAD1 A, Sig=300,4 Ref=400,10

Peak #	RetTime [min]	Type	Width [min]	Area [mAU*s]	Height [mAU]	Area %
1	6.895	MM	0.1019	93.40249	15.26987	1.1074
2	7.904	MM	0.1164	8108.01123	1161.14124	96.1274
3	8.179	MM	0.1122	233.23743	34.65784	2.7652

Totals : 8434.65115 1211.06895

Signal 2: DAD1 B, Sig=310,4 Ref=400,10

Peak #	RetTime [min]	Type	Width [min]	Area [mAU*s]	Height [mAU]	Area %
1	6.893	MM	0.1523	181.80042	19.89683	2.0865
2	7.904	MF	0.1147	8362.10840	1214.82483	95.9712
3	8.179	FM	0.0895	169.23830	31.51430	1.9423

Totals : 8713.14711 1266.23596

Signal 3: DAD1 C, Sig=320,4 Ref=400,10

Peak #	RetTime [min]	Type	Width [min]	Area [mAU*s]	Height [mAU]	Area %
1	6.893	MM	0.1620	172.31148	17.72326	2.1494
2	7.904	MF	0.1155	7637.97559	1101.79370	95.2740
3	8.179	FM	0.1095	206.56557	31.44277	2.5766

Totals : 8016.85263 1150.95973

Fig. S-6. Chromatogram for the assessment of the purity of compound **6**, with tables showing the detector response at three wavelengths.

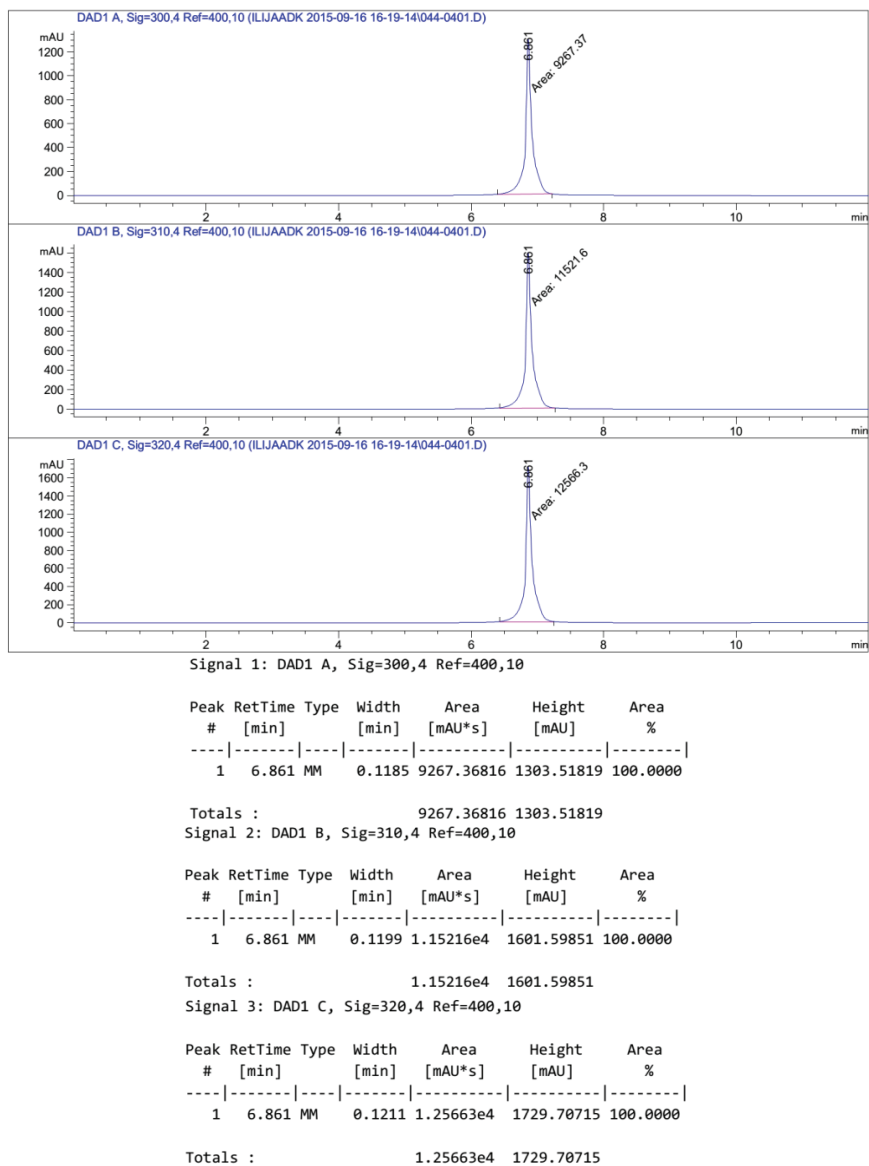


Fig. S-7. Chromatogram for the assessment of the purity of compound 7, with tables showing the detector response at three wavelengths.

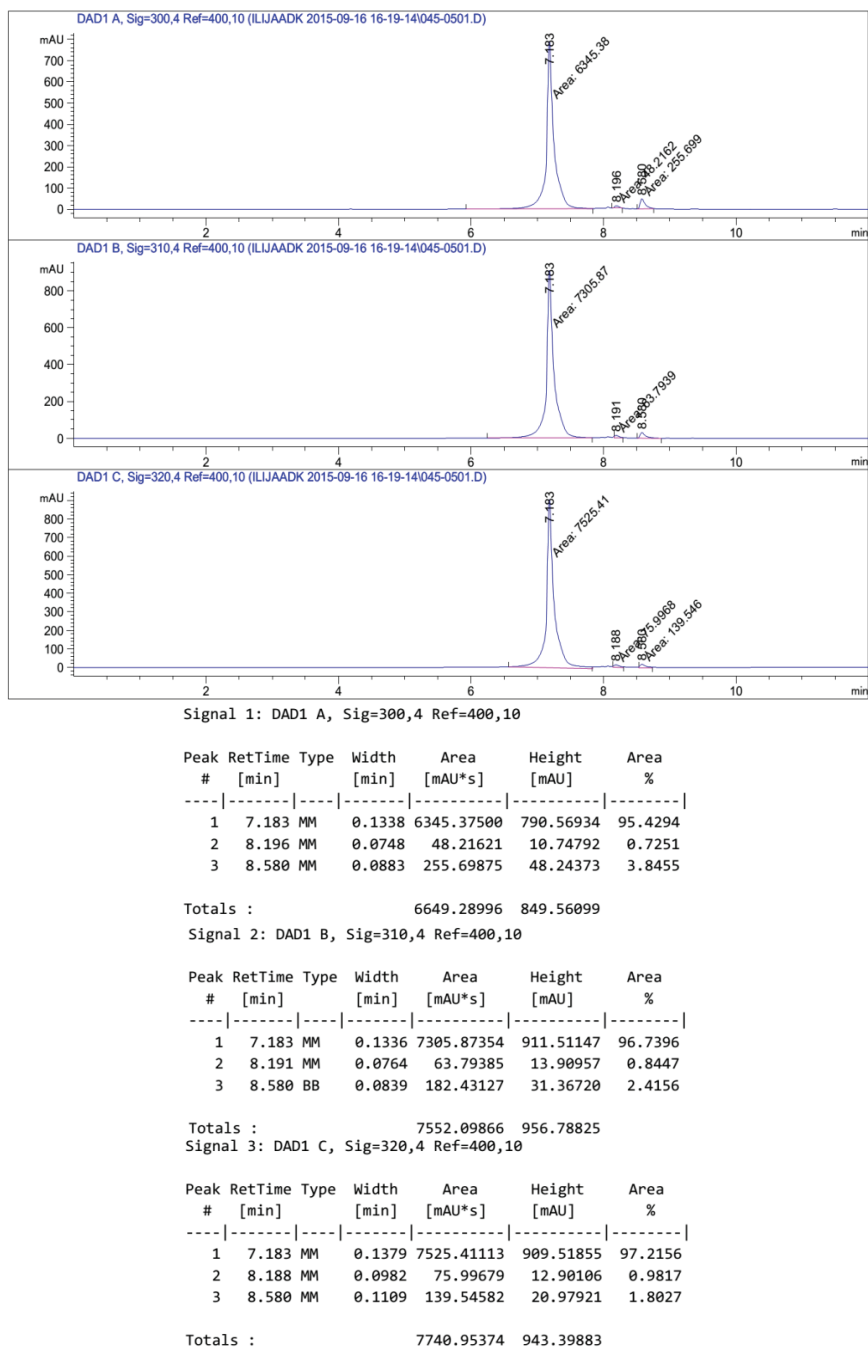
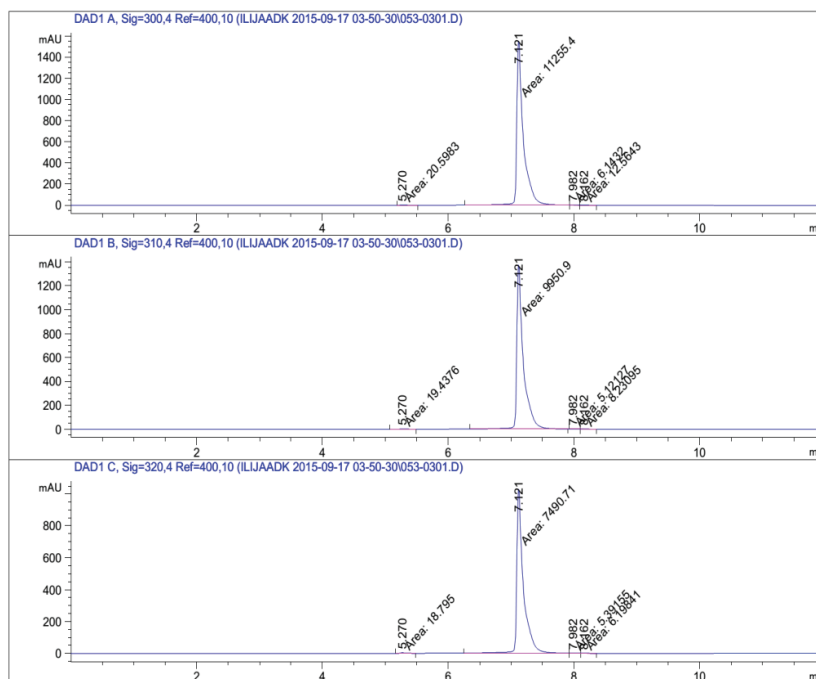


Fig. S-8. Chromatogram for the assessment of the purity of compound **8**, with tables showing the detector response at three wavelengths.



Peak #	RetTime [min]	Type	Width [min]	Area [mAU*s]	Height [mAU]	Area %
1	5.270	MM	0.1076	20.59832	3.18970	0.1824
2	7.121	MM	0.1205	1.12554e4	1556.25171	99.6520
3	7.982	MM	0.0917	6.14320	1.11701	0.0544
4	8.162	MM	0.1114	12.56429	1.87958	0.1112

Totals : 1.12947e4 1562.43800  
Signal 2: DAD1 B, Sig=310,4 Ref=400,10

Peak #	RetTime [min]	Type	Width [min]	Area [mAU*s]	Height [mAU]	Area %
1	5.270	MM	0.0926	19.43761	3.49813	0.1947
2	7.121	MM	0.1205	9950.90234	1375.92627	99.6716
3	7.982	MM	0.0745	5.12127	1.14633	0.0513
4	8.162	MM	0.0911	8.23095	1.50506	0.0824

Totals : 9983.69218 1382.07579  
Signal 3: DAD1 C, Sig=320,4 Ref=400,10

Peak #	RetTime [min]	Type	Width [min]	Area [mAU*s]	Height [mAU]	Area %
1	5.270	MM	0.0944	18.79499	3.31737	0.2499
2	7.121	MM	0.1210	7490.70850	1032.15369	99.5960
3	7.982	MM	0.0718	5.39155	1.25197	0.0717
4	8.162	MM	0.0935	6.19841	1.10505	0.0824

Totals : 7521.09344 1037.82807

Fig. S-9. Chromatogram for the assessment of the purity of compound **9**, with tables showing the detector response at three wavelengths.

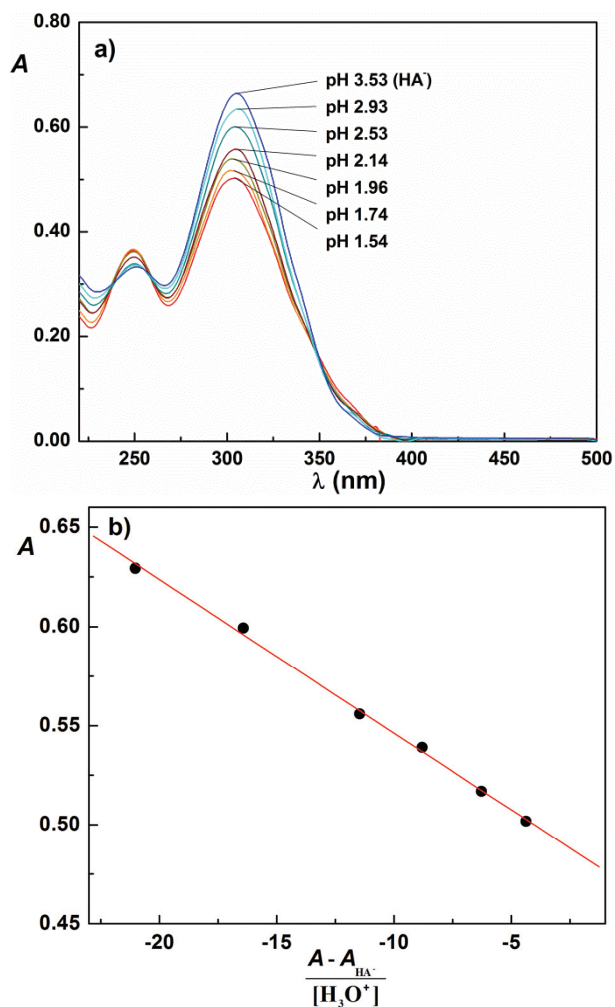


Fig. S-10. Absorption spectra of compound **2** used for  $K_{a1}$  determination in solutions of different acidity, the pH values are indicated; b) Spectrophotometric determination of  $K_{a1}$  according to Eq. (1);  $c_2 = 5.023 \times 10^{-5}$  M;  $\lambda = 302.9$  nm;  $t = 25$  °C,  $I = 0.1$  M (NaCl); scan speed  $500$  nm  $\text{min}^{-1}$ .

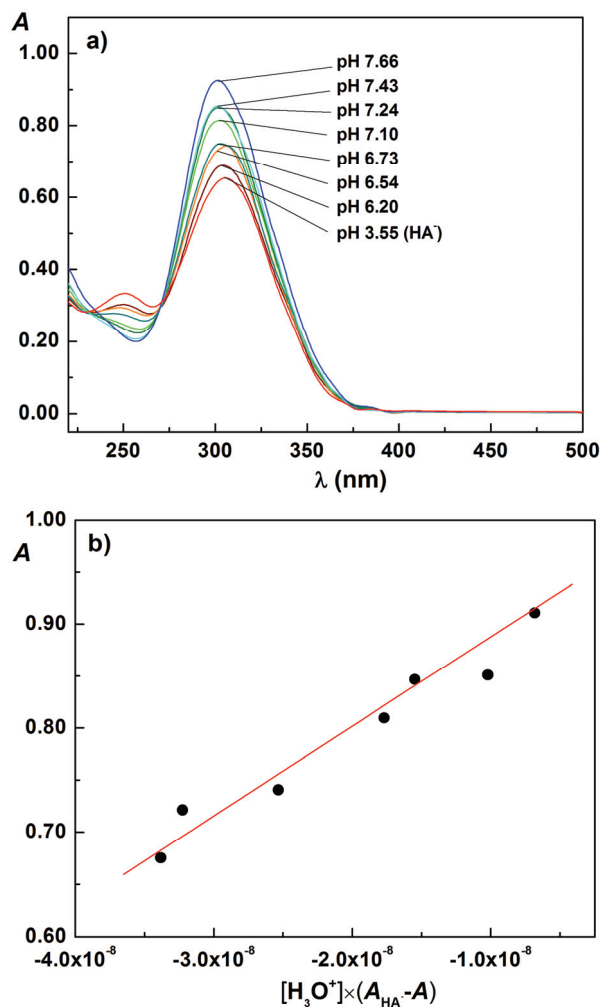


Fig. S-11. Absorption spectra of compound **2** used for  $K_{a2}$  determination in solutions of different acidity, the pH values are indicated; b) Spectrophotometric determination of  $K_{a2}$  according to Eq. (2);  $c_2 = 5.023 \times 10^{-5}$  M;  $\lambda = 299.5$  nm;  $t = 25$  °C,  $I = 0.1$  M (NaCl); scan speed  $500$  nm  $\text{min}^{-1}$ .

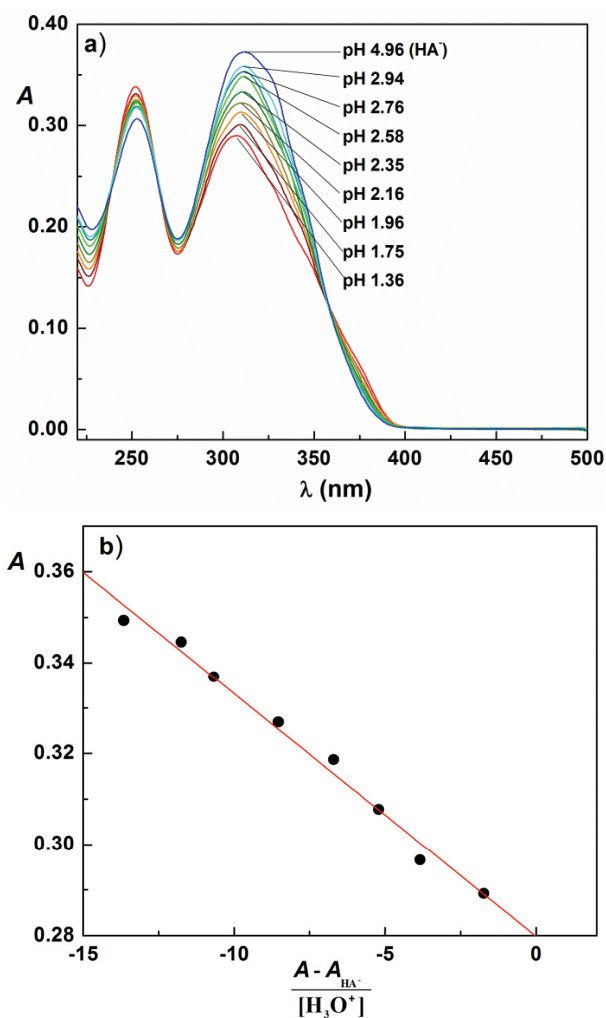


Fig. S-12. Absorption spectra of compound **3** used for  $K_{a1}$  determination in solutions of different acidity, the pH values are indicated; b) Spectrophotometric determination of  $K_{a1}$  according to Eq. (1);  $c_3 = 4.908 \times 10^{-5}$  M;  $\lambda = 305.4$  nm;  $t = 25$  °C,  $I = 0.1$  M (NaCl); scan speed  $500$  nm  $\text{min}^{-1}$ .

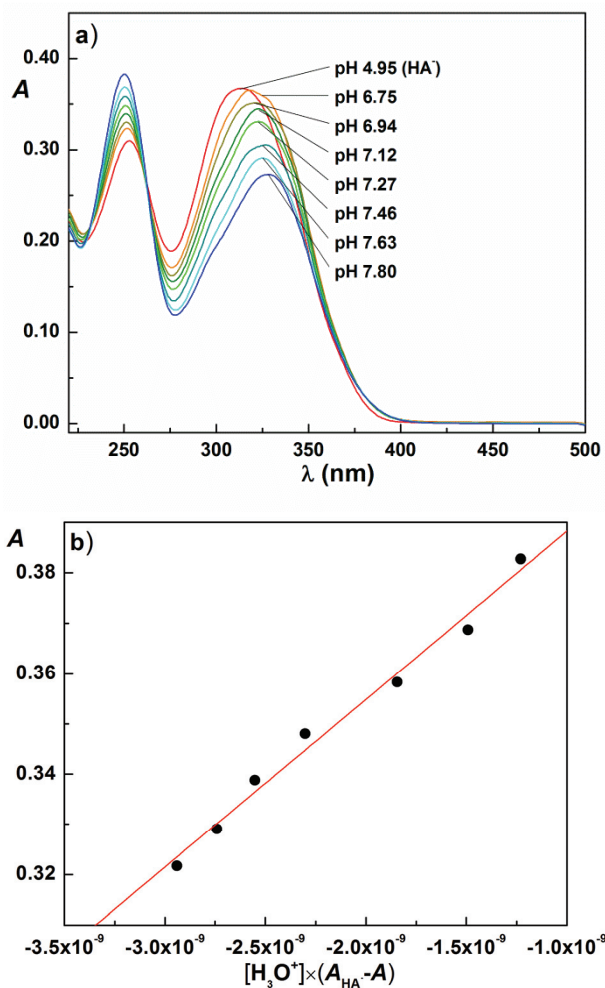


Fig. S-13. Absorption spectra of compound **3** used for  $K_{a2}$  determination in solutions of different acidity, the pH values are indicated; b) Spectrophotometric determination of  $K_{a2}$  according to Eq. (2);  $c_3 = 4.908 \times 10^{-5}$  M;  $\lambda = 250.0$  nm;  $t = 25$  °C,  $I = 0.1$  M (NaCl); scan speed  $500$  nm  $\text{min}^{-1}$ .



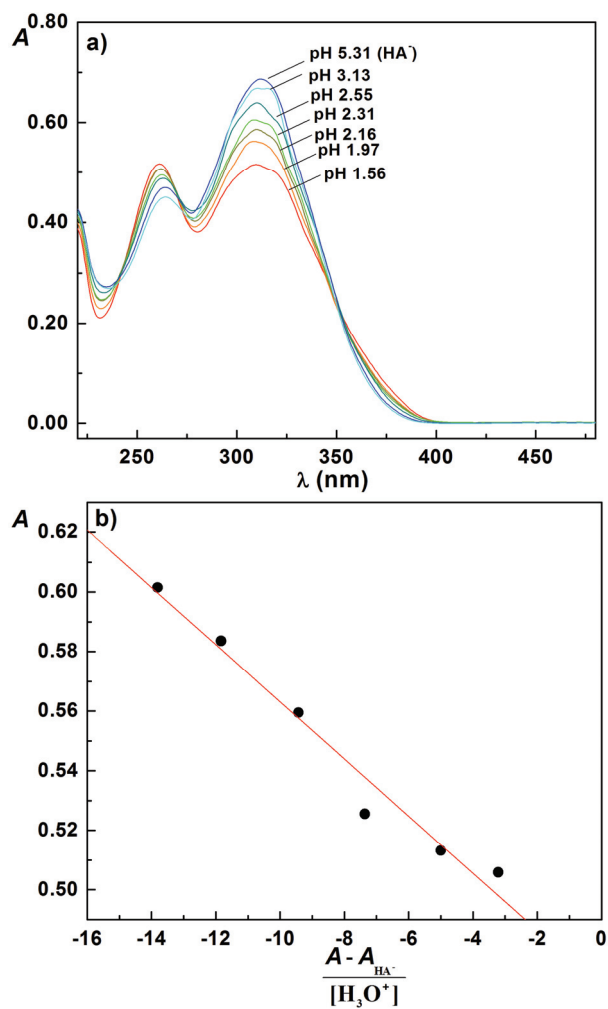


Fig. S-14. Absorption spectra of compound **5** used for  $K_{a1}$  determination in solutions of different acidity, the pH values are indicated; b) Spectrophotometric determination of  $K_{a1}$  according to Eq (1);  $c_5 = 6.021 \times 10^{-5}$  M;  $\lambda = 312.3$  nm;  $t = 25$  °C,  $I = 0.1$  M (NaCl); scan speed  $500$  nm  $\text{min}^{-1}$ .

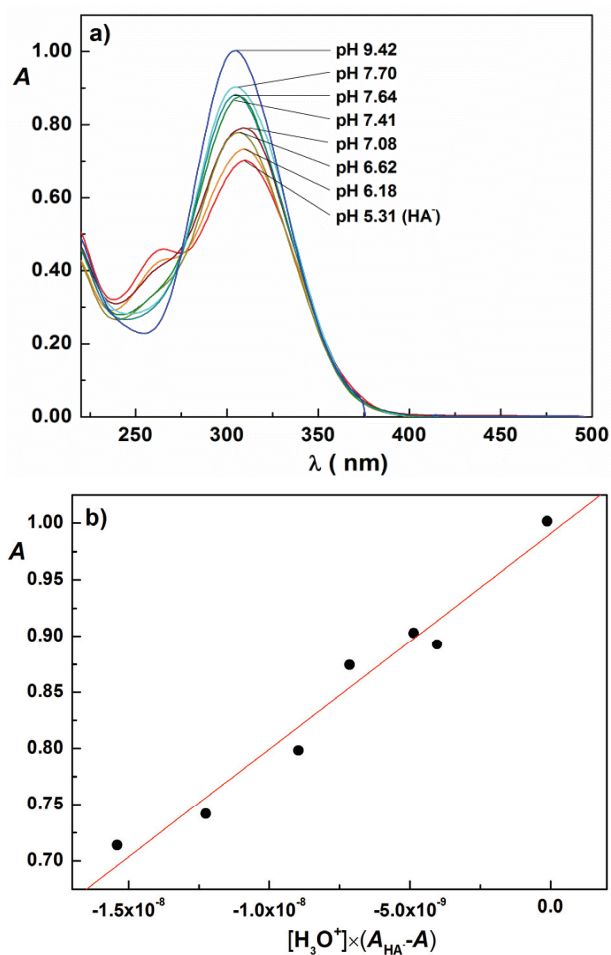


Fig. S-15. Absorption spectra of compound **5** used for  $K_{a2}$  determination in solutions of different acidity, the pH values are indicated; b) Spectrophotometric determination of  $K_{a2}$  according to Eq. (2);  $c_5 = 6.021 \times 10^{-5}$  M;  $\lambda = 305.9$  nm;  $t = 25$  °C,  $I = 0.1$  M (NaCl); scan speed  $500$  nm  $\text{min}^{-1}$ .

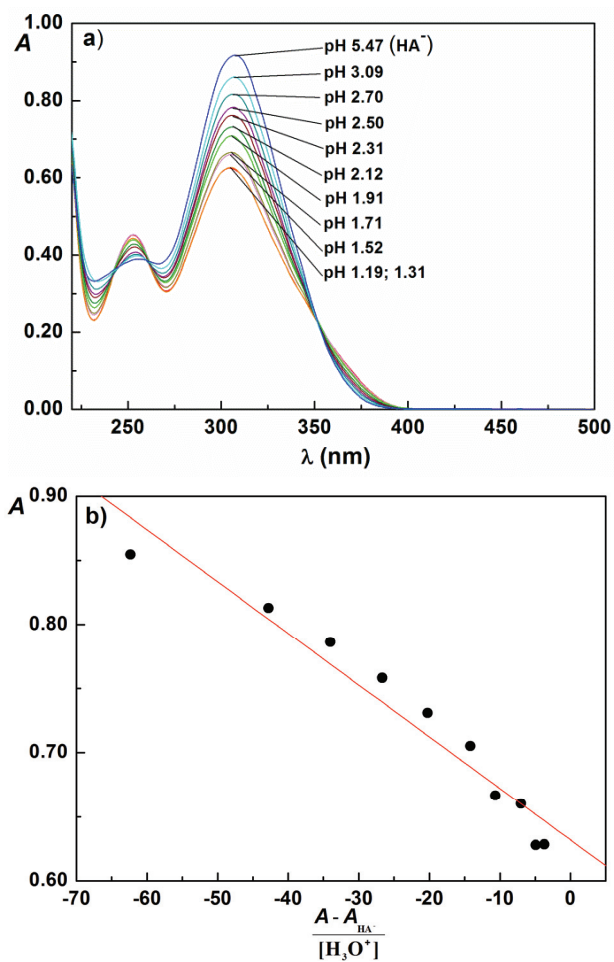


Fig. S-16. Absorption spectra of compound **6** used for  $K_{a1}$  determination in solutions of different acidity, the pH values are indicated; b) Spectrophotometric determination of  $K_{a1}$  according to Eq (1);  $c_6 = 9.014 \times 10^{-5}$  M;  $\lambda = 306.3$  nm;  $t = 25$  °C,  $I = 0.1$  M (NaCl); scan speed  $500$  nm  $\text{min}^{-1}$ .

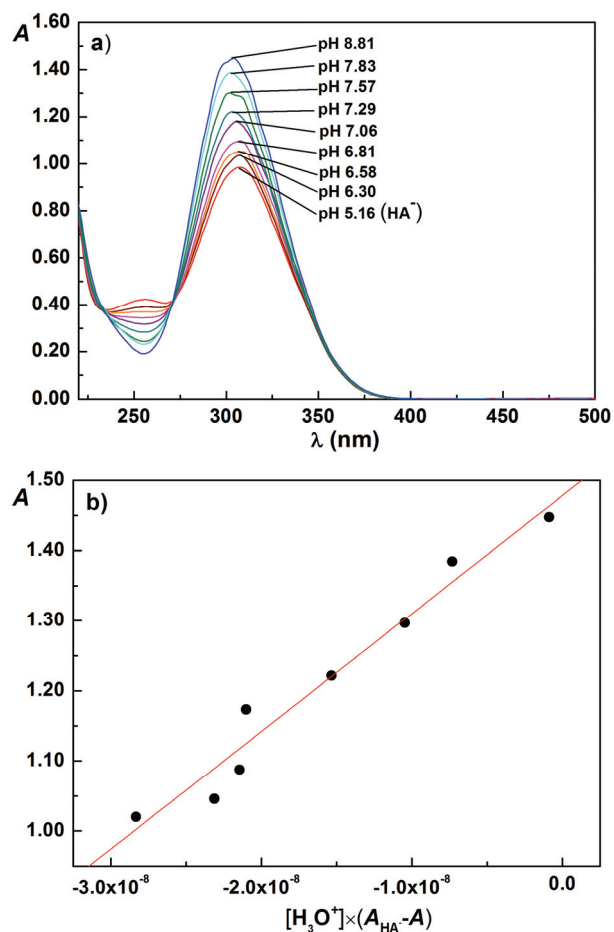


Fig. S-17. Absorption spectra of compound **6** used for  $K_{a2}$  determination in solutions of different acidity, the pH values are indicated; b) Spectrophotometric determination of  $K_{a2}$  according to Eq. (2);  $c_6 = 9.014 \times 10^{-5}$  M;  $\lambda = 303.7$  nm;  $t = 25$  °C,  $I = 0.1$  M (NaCl); scan speed  $500$  nm  $\text{min}^{-1}$ .

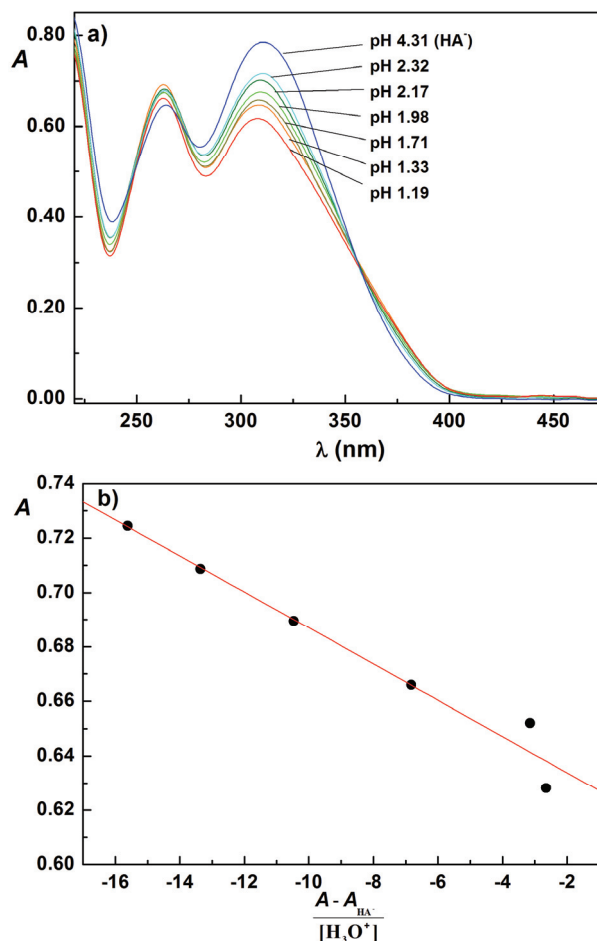


Fig. S-18. Absorption spectra of compound **8** used for  $K_{a1}$  determination in solutions of different acidity, the pH values are indicated; b) Spectrophotometric determination of  $K_{a1}$  according to Eq. (1);  $c_8 = 5.904 \times 10^{-5}$  M;  $\lambda = 308.8$  nm;  $t = 25$  °C,  $I = 0.1$  M (NaCl); scan speed  $500 \text{ nm min}^{-1}$ .

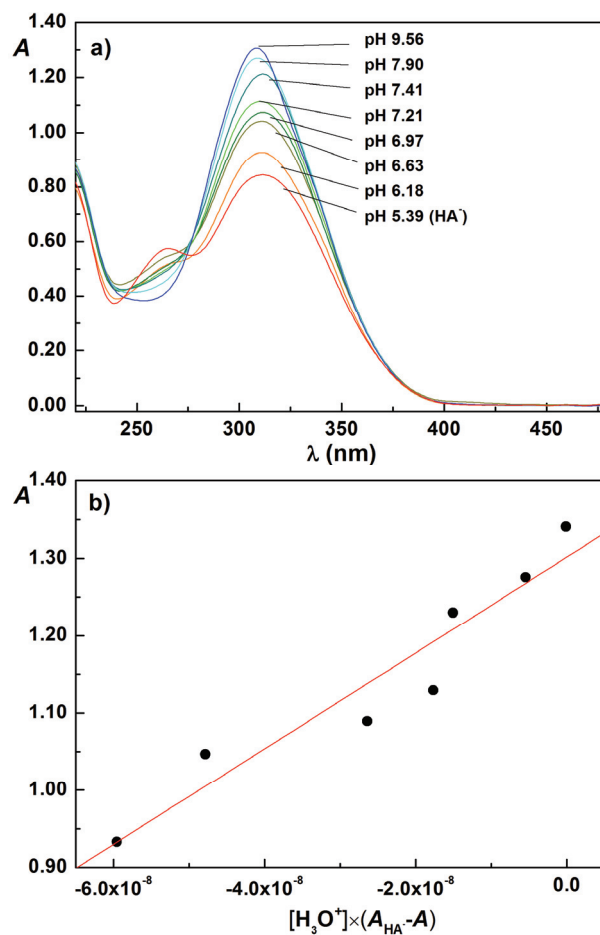


Fig. S-19. Absorption spectra of compound **8** used for  $K_{a2}$  determination in solutions of different acidity, the pH values are indicated; b) Spectrophotometric determination of  $K_{a2}$  according to Eq. (2);  $c_8 = 5.904 \times 10^{-5}$  M;  $\lambda = 308.0$  nm;  $t = 25$  °C,  $I = 0.1$  M (NaCl); scan speed  $500$  nm  $\text{min}^{-1}$ .

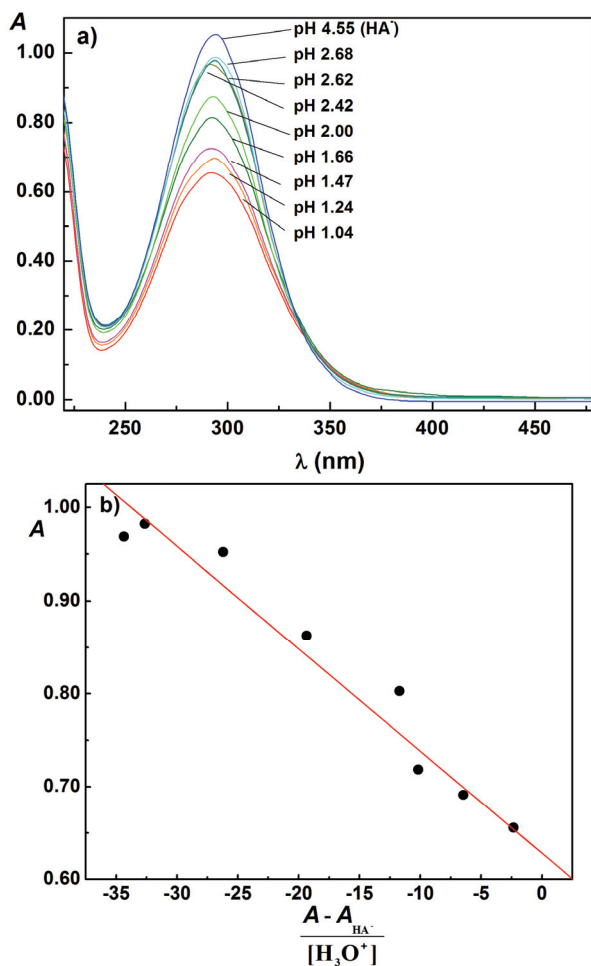


Fig. S-20. Absorption spectra of compound **9** used for  $K_{a1}$  determination in solutions of different acidity, the pH values are indicated; b) Spectrophotometric determination of  $K_{a1}$  according to Eq. (1);  $c_9 = 6.066 \times 10^{-5}$  M;  $\lambda = 293.0$  nm;  $t = 25$  °C,  $I = 0.1$  M (NaCl); scan speed  $500$  nm  $\text{min}^{-1}$ .

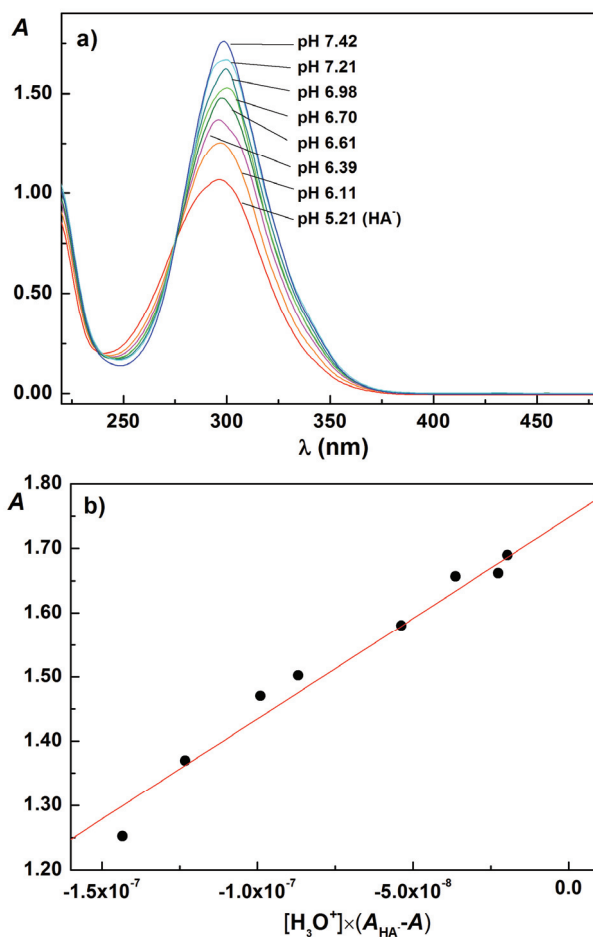


Fig. S-21. Absorption spectra of compound **9** used for  $K_{a2}$  determination in solutions of different acidity, the pH values are indicated; b) Spectrophotometric determination of  $K_{a2}$  according to Eq. (2);  $c_9 = 6.066 \times 10^{-5}$  M;  $\lambda = 296.0$  nm;  $t = 25$  °C,  $I = 0.1$  M (NaCl); scan speed  $500$  nm  $\text{min}^{-1}$ .



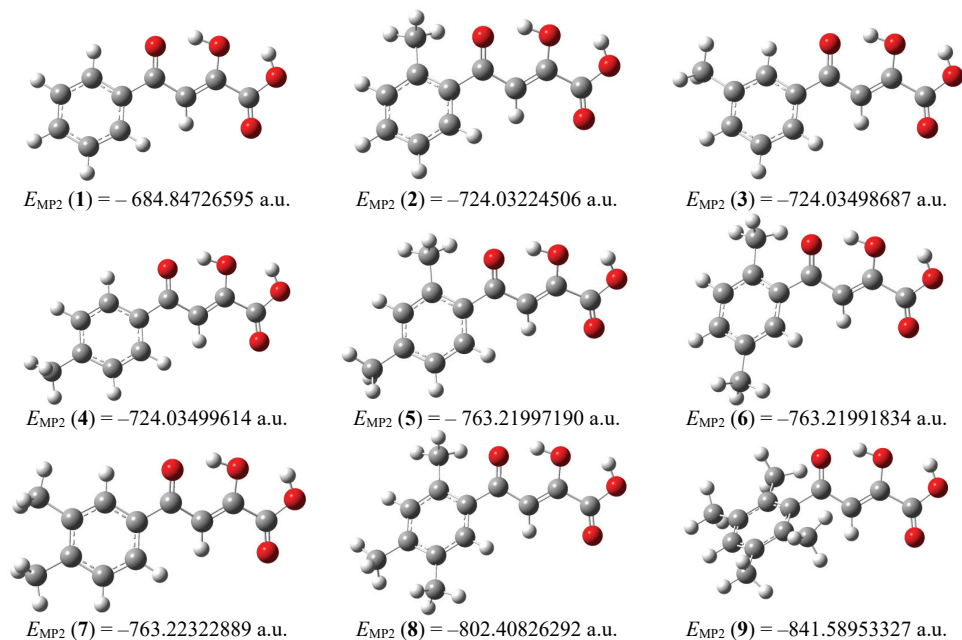


Fig. S-22. Optimized geometries and energies of 1–9 in their molecular ( $H_2A$ ) form; MP2/6-31g (d,p) with PCM water solvation.

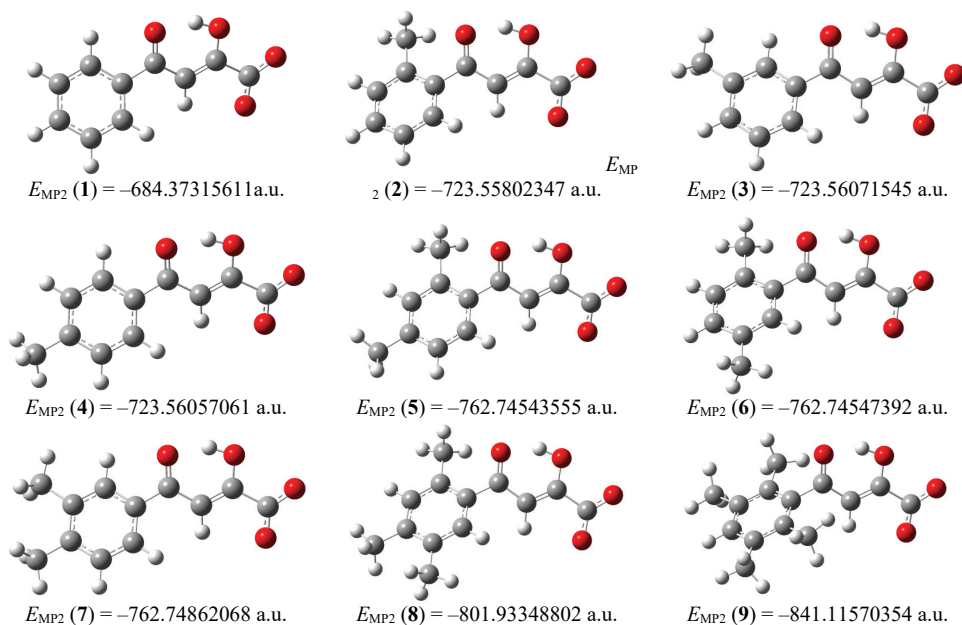


Fig. S-23. Optimized geometries and energies of 1–9 in their monoanionic ( $HA^-$ ) form; MP2/6-31g (d,p) with PCM water solvation.

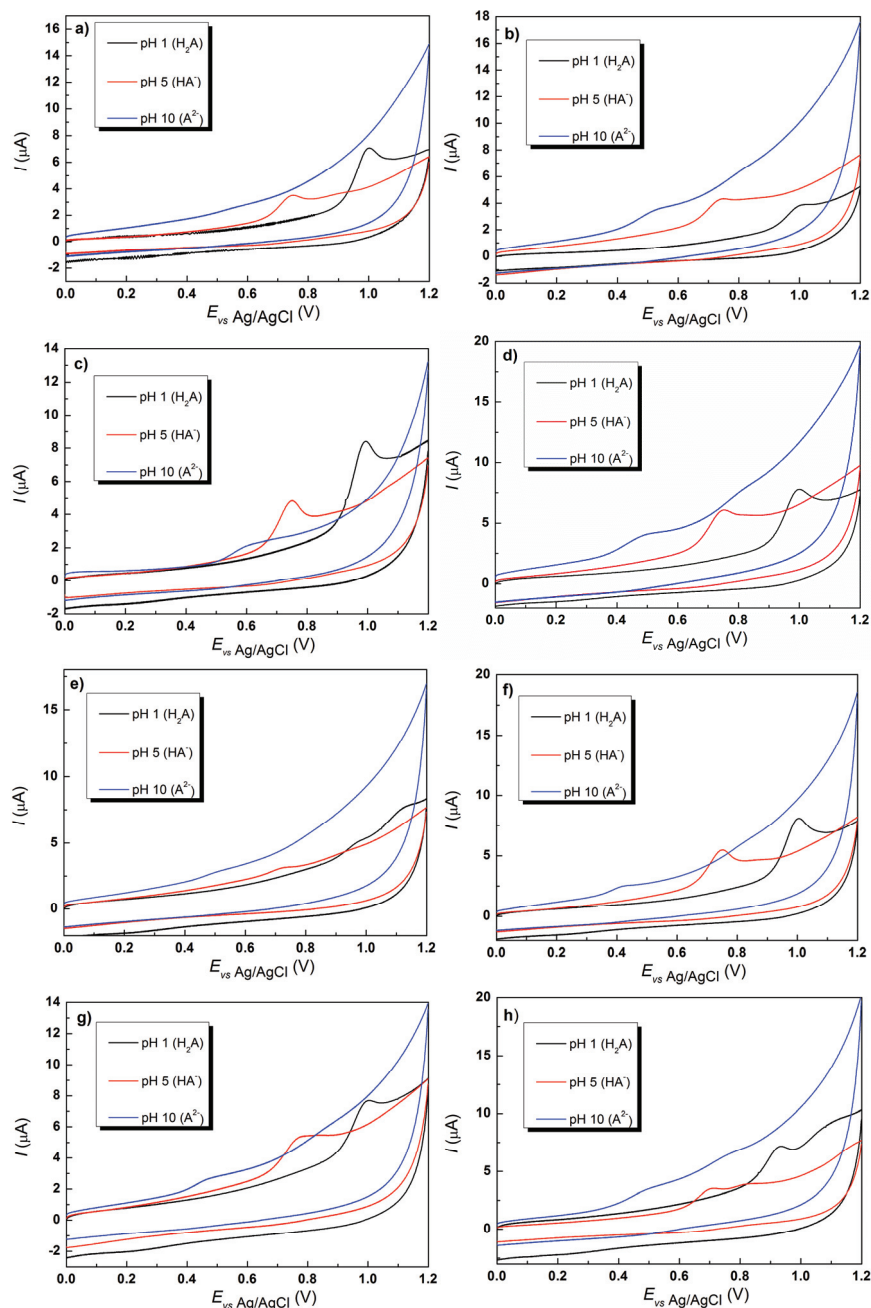


Fig. S-24. Cyclic voltammograms of compounds **1–3** and **5–9** in Britton–Robinson buffer at pH 1, pH 5, and pH 10. a) **1**,  $c_1 = 5.46 \times 10^{-5}$  M; b) **2**,  $c_2 = 4.61 \times 10^{-5}$  M; c) **3**,  $c_3 = 6.54 \times 10^{-5}$  M; d) **5**,  $c_5 = 6.58 \times 10^{-5}$  M; e) **6**,  $c_6 = 4.09 \times 10^{-5}$  M; f) **7**,  $c_7 = 5.22 \times 10^{-5}$  M; g) **8**,  $c_8 = 4.06 \times 10^{-5}$  M; h) **9**,  $c_9 = 4.43 \times 10^{-5}$  M; scan rate  $100 \text{ mV s}^{-1}$ ,  $t = 25 \pm 1$  °C.

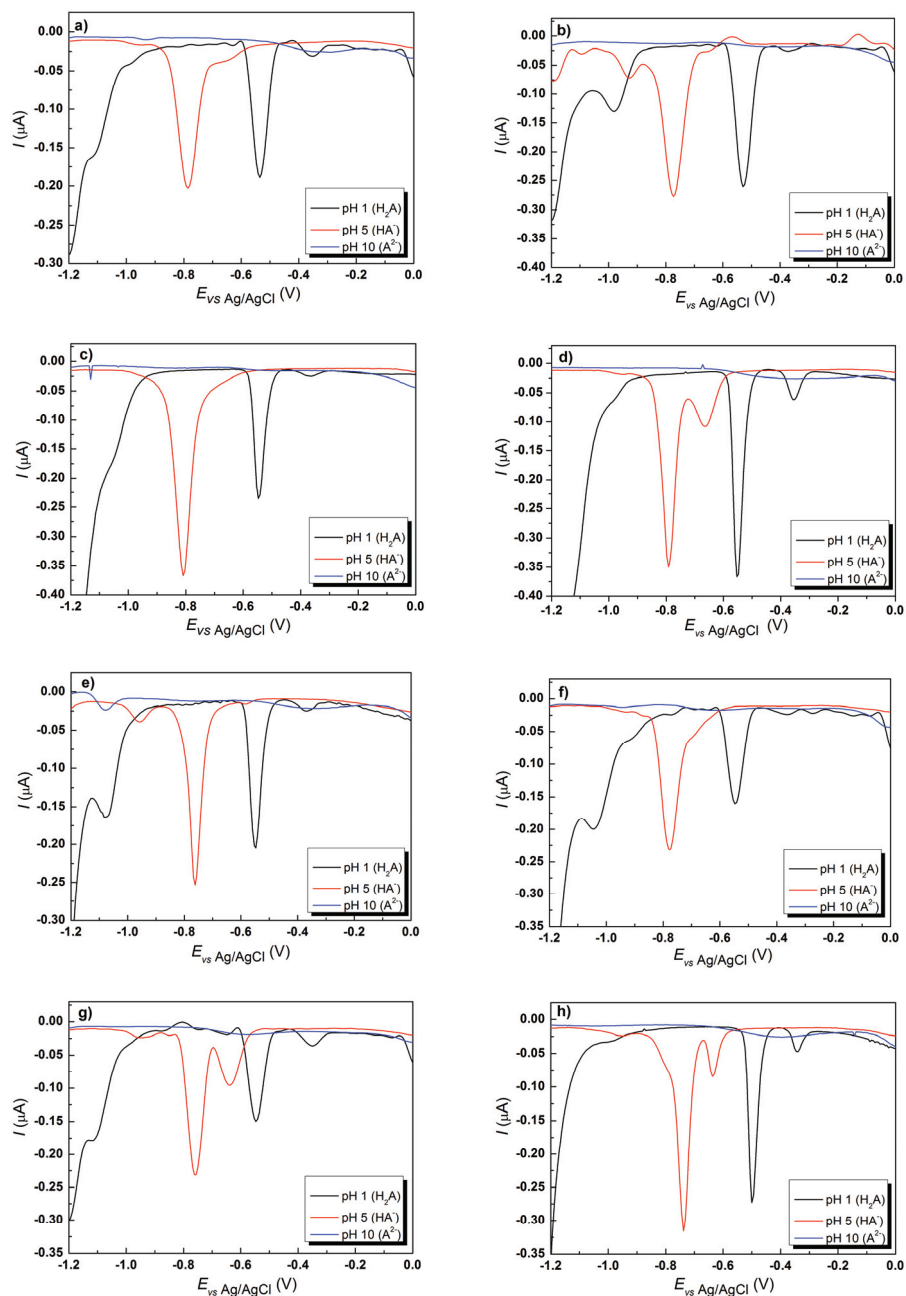


Fig. S-25. Differential pulse polarograms of compound 2–9 in Britton–Robinson buffer at pH 1, pH 5, and pH 10; a) 2,  $c_2 = 4.61 \times 10^{-5}$  M; b) 3,  $c_3 = 6.54 \times 10^{-5}$  M; c) 4,  $c_4 = 4.77 \times 10^{-5}$  M; d) 5,  $c_5 = 6.58 \times 10^{-5}$  M; e) 6,  $c_6 = 4.09 \times 10^{-5}$  M; f) 7,  $c_7 = 5.22 \times 10^{-5}$  M; g) 8,  $c_8 = 4.06 \times 10^{-5}$  M; h) 9,  $c_9 = 4.43 \times 10^{-5}$  M; scan rate  $13 \text{ mV s}^{-1}$ ,  $t = 25 \pm 1$  °C.

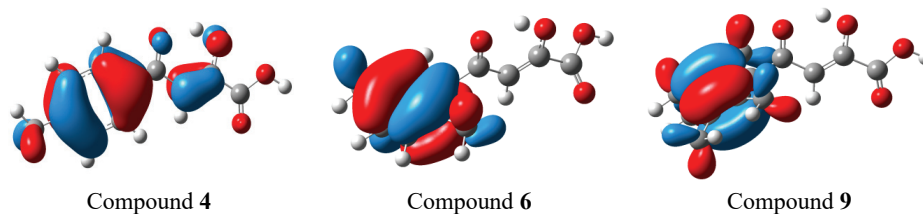


Fig. S-26. HOMO orbitals of the H<sub>2</sub>A form of compounds **4**, **6** and **9** plotted on the isocontour level 0.03.

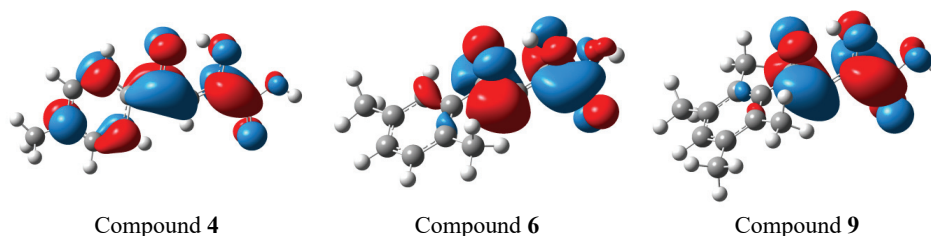


Fig. S-27. LUMO orbitals of the H<sub>2</sub>A form of compounds **4**, **6** and **9** plotted on the isocontour level 0.03.

TABLE S-I. Energies of the FMOs (given in Hartree), and dipoles (given in Debye) for the molecular and monoanionic forms of compounds **1–9**

Compound	Neutral (H <sub>2</sub> A)				Anion (HA <sup>-</sup> )			
	HOMO	LUMO	HOMO/ LUMO gap	Dipole	HOMO	LUMO	HOMO/ LUMO gap	Dipole
<b>1</b>	-0.3470	0.0367	0.3837	2.7040	-0.3321	0.0625	0.3946	20.1289
<b>2</b>	-0.3359	0.0406	0.3764	2.3366	-0.3274	0.0670	0.3944	20.7147
<b>3</b>	-0.3363	0.0377	0.3740	2.8168	-0.3266	0.0625	0.3891	22.3967
<b>4</b>	-0.3360	0.0394	0.3754	3.2365	-0.3244	0.0641	0.3885	22.8528
<b>5</b>	-0.3299	0.0417	0.3716	2.8786	-0.3213	0.0683	0.3896	23.1538
<b>6</b>	-0.3236	0.0401	0.3638	2.6851	-0.3172	0.0670	0.3842	21.9031
<b>7</b>	-0.3300	0.0403	0.3703	3.3452	-0.3199	0.0641	0.3840	24.8252
<b>8</b>	-0.3196	0.0425	0.3621	3.1584	-0.3129	0.0687	0.3816	24.0766
<b>9</b>	-0.3100	0.0448	0.3548	2.4134	-0.3063	0.0778	0.3840	22.9021

Table S-II. Energies of the FMOs (given in Hartree), and dipole moments (given in Debye) for the radical anions and radical cations derived from molecular form ( $H_2A$ ) or monoanionic form ( $HA^-$ ) of compounds **1–9**. Energies of  $\alpha$ SOMO and  $\alpha$ LUMO are shown.

Compound	Radical anion from $H_2A$				Radical cation from $H_2A$			
	SOMO	LUMO	SOMO/ LUMO gap	Dipole	SOMO	LUMO	SOMO/ LUMO gap	Dipole
<b>1</b>	0.0757	0.2471	0.1713	5.1253	-0.3009	-0.1600	0.1409	2.2888
<b>2</b>	0.0767	0.2475	0.1708	5.6837	-0.2996	-0.1579	0.1417	3.0584
<b>3</b>	0.0756	0.2459	0.1703	6.6132	-0.2989	-0.1576	0.1413	3.3480
<b>4</b>	0.0765	0.2458	0.1693	7.3901	-0.2970	-0.1551	0.1419	2.9073
<b>5</b>	0.0774	0.2465	0.1691	7.7582	-0.2761	-0.1313	0.1449	2.9050
<b>6</b>	0.0766	0.2443	0.1677	7.0045	-0.2975	-0.1555	0.1421	3.4272
<b>7</b>	0.0763	0.2452	0.1690	8.6434	-0.2749	-0.1306	0.1443	3.1645
<b>8</b>	0.0772	0.2461	0.1689	8.8467	-0.2751	-0.1316	0.1435	1.9357
<b>9</b>	0.0784	0.2537	0.1754	8.6062	-0.2532	-0.0821	0.1711	10.3233
Compound	Radical dianion from $HA^-$							
	SOMO	LUMO	SOMO/ LUMO gap	Dipole				
<b>1</b>	0.1658	0.3866	0.2208	12.3478				
<b>2</b>	0.1685	0.3824	0.2138	14.5640				
<b>3</b>	0.1641	0.3836	0.2195	15.5722				
<b>4</b>	0.1645	0.3812	0.2167	15.8690				
<b>5</b>	0.1669	0.3779	0.2109	17.5080				
<b>6</b>	0.1664	0.3836	0.2172	16.0213				
<b>7</b>	0.1631	0.3817	0.2186	18.6586				
<b>8</b>	0.1665	0.3795	0.2130	19.1801				
<b>9</b>	0.1875	0.3529	0.1654	23.1287				

Table S-III. Intercorrelation matrix ( $r$  values) between oxidation/reduction potentials at pH 1 and at pH 5 and the descriptors extracted from QM calculations. The indicator variable ( $I$ ) is also included. ‘molecular’ refers to the neutral form of the compounds; ‘anion’ refers to the anionic form of the compounds (deprotonated carboxyl group); ‘RA’ refers to the radical anion/dianion (derived from the neutral/anionic form); ‘RC’ refers to the radical cation derived from the neutral form

$E_{ox} - pH_{-1}$		$E_{red} - pH_{-1}$	
HOMO (molecular)	-0.6797	HOMO (molecular)	0.3250
LUMO (molecular)	-0.5739	LUMO molecular	0.2916
HOMO/LUMO gap (molecular)	0.6876	HOMO/LUMO gap (molecular)	-0.3233
Dipole (molecular)	0.3642	Dipole (molecular)	-0.6104
SOMO (RC)	-0.6565	SOMO (RA)	0.3298
LUMO (RC)	-0.7924	LUMO (RA)	0.8713
SOMO/LUMO gap (RC)	-0.9352	SOMO/LUMO gap (RA)	0.9361
Dipole (RC)	-0.9519	Dipole (RA)	-0.0503
$I$	-0.7908	$I$	0.5906

Table S-III. Continued

$E_{\text{ox}} - \text{pH}_5$		$E_{\text{red}} - \text{pH}_5$	
HOMO (molecular)	-0.4092	HOMO (anion)	0.8213
LUMO (molecular)	-0.3958	LUMO (anion)	0.7433
HOMO/LUMO gap (molecular)	0.3999	HOMO/LUMO gap (anion)	-0.6495
Dipole (molecular)	0.4117	Dipole (molecular)	-0.3518
SOMO (RC)	-0.4353	SOMO dianion (RA)	0.6858
LUMO (RC)	-0.6048	LUMO dianion (RA)	-0.6739
SOMO/LUMO gap (RC)	-0.8283	SOMO/LUMO gap dianion (RA)	-0.6869
Dipole (RC)	-0.9067	Dipole of dianion (RA)	0.7311
<i>I</i>	-0.5295	<i>I</i>	0.9533